Stomatal immunity against fungal invasion comprises not only chitin-induced stomatal closure but also chitosan-induced guard cell death

Wenxiu Ye[a,b,c,1], Shintaro Munemasa[b], Tomonori Shinya[d], Wei Wu[a], Tao Ma[a], Jiang Lu[a], Toshinori Kinoshita[c,e], Hanae Kaku[f], Naoto Shibuya[f], and Yoshiyuki Murata[b,1]

[a]School of Agriculture and Biology, Shanghai Jiao Tong University, Minhang, 200240 Shanghai, China; [b]Graduate School of Environmental and Life Science, Okayama University, Tsushima-Naka, 700-8530 Okayama, Japan; [c]Institute of Transformative Bio-Molecules, Nagoya University, Chikusa, 464-8602 Nagoya, Japan; [d]Institute of Plant Science and Resources, Okayama University, Kurashiki, 710-0046 Okayama, Japan; [e]Graduate School of Science, Nagoya University, Chikusa, 464-8602 Nagoya, Japan; and [f]Department of Life Sciences, School of Agriculture, Meiji University, Kawasaki, 214-8571 Kanagawa, Japan

Edited by Natasha V. Raikhel, Center for Plant Cell Biology, Riverside, CA, and approved July 14, 2020 (received for review December 21, 2019)

Many pathogenic fungi exploit stomata as invasion routes, causing destructive diseases of major cereal crops. Intensive interaction is expected to occur between guard cells and fungi. In the present study, we took advantage of well-conserved molecules derived from the fungal cell wall, chitin oligosaccharide (CTOS), and chitosan oligosaccharide (CSOS) to study how guard cells respond to fungal invasion. In *Arabidopsis*, CTOS induced stomatal closure through a signaling mediated by its receptor CERK1, Ca^{2+}, and a major S-type anion channel, SLAC1. CSOS, which is converted from CTOS by chitin deacetylases from invading fungi, did not induce stomatal closure, suggesting that this conversion is a fungal strategy to evade stomatal closure. At higher concentrations, CSOS but not CTOS induced guard cell death in a manner dependent on Ca^{2+} but not CERK1. These results suggest that stomatal immunity against fungal invasion comprises not only CTOS-induced stomatal closure but also CSOS-induced guard cell death.

Ca^{2+} signaling | chitin oligosaccharide | chitosan oligosaccharide | fungal resistance | stomatal immunity

Stomata, surrounded by pairs of guard cells, regulate gas exchange between plants and the environment, thus being critical for plant growth. On the other hand, a variety of bacteria, oomycetes, and fungi exploit stomatal openings as major invasion routes (1, 2). To prevent microbe invasion, plants can recognize the so-called microbe-associated molecular patterns (MAMPs) that are highly conserved in the whole class of microbes, such as flagellin for bacteria and chitin oligosaccharides (CTOSs) for fungi, leading to stomatal immunity or stomatal defense, including stomatal closure and inhibition of stomatal opening (3–5). Recent studies have focused on bacterium–guard cell interaction and found that pathogenic bacteria secrete phytotoxins and proteins, termed as effectors, to suppress bacterial MAMP-induced stomatal immunity (3–5). Although many pathogenic fungi penetrate through stomata, posing major threats to crop production and consequently human nutrition, the fungus–guard cell interaction mechanism is much less understood.

Among the fungi penetrating through stomata, rust fungi are notorious for causing many destructive diseases of major cereal crops, such as wheat, maize, and barley (6). In an interaction between a wheat leaf rust fungus and *Arabidopsis*, it has been observed that penetration of the rust fungi induced a transient stomatal closure, followed by the hypersensitive response of guard cells causing guard cell death that eventually prevented the fungal infection (7). Although the details of the molecular mechanism remain unknown, these results suggest that guard cells actively respond to rust fungal invasion even in the form of suicide.

Chitin, an insoluble polymer of β-1,4-linked *N*-acetylglucosamine, is a major component of the fungal cell wall. During fungal invasion, plant chitinases (Enzyme Commission [EC] 3.2.1.14) hydrolyze chitin, releasing CTOS that triggers plant immune responses, mediated by a receptor complex formed by lysin motif (LysM)-type receptor-like kinases, lysin motif receptor kinase 5 (LYK5), and Chitin Elicitor Receptor Kinase 1 (CERK1), in *Arabidopsis* (8, 9). To suppress plant immune responses, many fungi secrete chitin de-N-acetylases (EC 3.5.1.41) to convert chitin to chitosan, a poor substrate of chitinases, avoiding cell wall degradation, and CTOS to chitosan oligosaccharide (CSOS) (10, 11). Fully deacetylated CSOS does not bind to the CTOS receptor or induce immune responses, including production of reactive oxygen species (ROS) and activation of mitogen-associated protein kinases (MAPKs) in *Arabidopsis* (12, 13). Thus, conversion of CTOS to CSOS is thought to dampen plant immune responses against fungal invasion.

Recent studies have observed CTOS-induced stomatal closure in *Arabidopsis* (14), but the molecular mechanism remains largely unknown. It is known that rust fungi secrete chitin deacetylases when they contact with guard cells intimately (10, 15). These results led us to hypothesize that conversion of CTOS to CSOS is a strategy for rust fungi to evade CTOS-induced stomatal immunity. However, guard cell responses to CSOS remain largely unclarified.

Significance

Fungal disease is a major threat to agriculture and consequently human nutrition. Many pathogenic fungi penetrate through stomata. This study reveals that chitin oligosaccharide (CTOS) from fungal cell wall induces stomatal closure through its receptor CERK1, Ca^{2+}, and S-type anion channel SLAC1, which would prevent fungal penetration. It is also shown that conversion of CTOS to chitosan oligosaccharide (CSOS) is a possible fungal strategy to circumvent stomatal immunity. At higher concentration, guard cells perceive CSOS, resulting in guard cell death, which potentially contributes to plant defense halting fungal infection through stomata. The finding of active guard cell death represents a conceptual advance in understanding of stomatal immunity and would guide future research on guard cell–microbe interaction and crop protection.

Author contributions: W.Y., S.M., T.S., N.S., and Y.M. designed research; W.Y., S.M., W.W., and T.M. performed research; W.Y., J.L., T.K., H.K., N.S., and Y.M. contributed new reagents/analytic tools; W.Y., S.M., W.W., T.M., and Y.M. analyzed data; and W.Y., N.S., and Y.M. wrote the paper.

The authors declare no competing interest.

This article is a PNAS Direct Submission.

[1]To whom correspondence may be addressed. Email: yewenxiu@sjtu.edu.cn or muta@cc.okayama-u.ac.jp.

This article contains supporting information online at https://www.pnas.org/lookup/suppl/doi:10.1073/pnas.1922319117/-/DCSupplemental.

First published August 10, 2020.

Cytosolic Ca^{2+} is a critical second messenger in stomatal movement (16–18). The influx of Ca^{2+} from the apoplast is mediated by Ca^{2+}-permeable cation channels (I_{Ca} channels) that are activated by plasma membrane hyperpolarization (19–22). Elevation of free cytosolic Ca^{2+} concentration ($[Ca^{2+}]_{cyt}$) is critical for S-type anion channel activation in guard cells (23–25). Further studies show that Ca^{2+}-dependent protein kinase 6 (CPK6) and a Ca^{2+}-independent protein kinase, Open Stomata 1 (OST1), are important for stomatal closure and activation of S-type anion channels in guard cells (25–33). In addition to stomatal movement, Ca^{2+} is also an important second messenger in signaling leading to plant cell death (34, 35).

In this study, we investigated CTOS signaling in guard cells and guard cell responses to CSOS in *Arabidopsis* to clarify the molecular basis for the interaction between guard cells and fungi.

Results

$(GlcNAc)_8$ but Not $(GlcN)_8$ Induces Stomatal Closure Mediated by CERK1. In *Arabidopsis*, CTOSs have different activity in inducing immune responses, with consistent activity seen for oligomers longer than hexamer (12, 36). Here, we investigated the effect of a bioactive CTOS, chitin octaose [$(GlcNAc)_8$], and its fully deacetylated counterpart, chitosan octaose [$(GlcN)_8$], on stomatal aperture. $(GlcNAc)_8$ induced stomatal closure in Col-0 in a dose-dependent manner, with a half maximal effective concentration (EC_{50}) of 15.07 μM, whereas $(GlcN)_8$ at similar concentrations did not affect stomatal apertures significantly (Fig. 1 and *SI Appendix*, Fig. S1*A*). Considering that the binding affinity of CTOS to its receptors is in the range of micromolar (36, 37), it can be suggested the concentration at micromolar for CTOS-induced stomatal closure is physiologically relevant.

Although $(GlcNAc)_8$ induced stomatal closure in leaf discs, $(GlcNAc)_8$ had little effect on transpirational water loss from detached leaves (*SI Appendix*, Fig. S2). On the other hand, abscisic acid (ABA) significantly reduced water loss from detached leaves (*SI Appendix*, Fig. S2). The distinct effects of ABA and $(GlcNAc)_8$ on transpirational water loss are probably due to a difference in water vapor in the substomatal cavity through certain limiting processes inside the leaf.

We next investigated the role of CTOS receptors CERK1, LYK5, and LYK4, the closest homolog of LYK5, in CTOS guard cell signaling. $(GlcNAc)_8$-induced stomatal closure was impaired in loss-of-function mutants *cerk1-2* and *cerk1-1* (Fig. 1*C*). A recent study reported that CERK1 is required for stomatal closure induced by a crude chitin preparation (38). In the present study, further results show that the defective phenotypes of *cerk1-2* and *cerk1-1* were complemented with the expression of CERK1 complementary DNA (cDNA) driven by the CaMV35S promoter (*35S CERK1*) and genomic fragment of CERK1 driven by the 1.1-kilobase (kb) native promoter sequence (*gCERK1*), respectively (Fig. 1*C*). Note that *35S CERK1* plants showed a more than 20-fold higher transcript level of *CERK1* (*SI Appendix*, Fig. S3*A*) but responded normally as wild type to $(GlcNAc)_8$ ($P = 0.31$). The *35S CERK1* plants also showed normal CTOS responses, such as ROS production and regulation of transcription (39). These results suggest that CERK1 is essential but not rate-limiting for $(GlcNAc)_8$-induced stomatal closure in *Arabidopsis*. $(GlcNAc)_8$-induced stomatal closure was not significantly affected by the loss-of-function of mutations *lyk4* and *lyk5* (*SI Appendix*, Fig. S3 *B* and *E*), which may be attributed to the redundancy of LYK4 and LYK5 (37).

In the following studies, we focused on functional analysis of *cerk1-2*, which is widely used for elucidating CTOS signaling (12, 37, 40). Application of 1 mM Ca^{2+} significantly induced stomatal closure in *cerk1-2* (*SI Appendix*, Fig. S3*C*), which indicates that stomata in *cerk1-2* are functional.

$(GlcNAc)_8$ Activates I_{Ca} Channels and Induces $[Ca^{2+}]_{cyt}$ Elevations Mediated by CERK1 in Guard Cells. Since Ca^{2+} influx mediated by I_{Ca} channels and the subsequent $[Ca^{2+}]_{cyt}$ elevations are critical in stomatal movement (4, 18, 41), we investigated the effect of $(GlcNAc)_8$ on I_{Ca} channels in guard cell protoplasts (GCPs) using the path-clamp technique and $[Ca^{2+}]_{cyt}$ in guard cells expressing a Ca^{2+} reporter, yellow chameleon 3.6 (YC3.6). $(GlcNAc)_8$ significantly activated I_{Ca} channel currents in Col-0 GCPs, which was impaired by the application of Ca^{2+} channel inhibitor, La^{3+} (Fig. 2). Further results show that the activation was impaired in *cerk1-2* GCPs, which was complemented by *35S CERK1* (Fig. 2). These results indicate that $(GlcNAc)_8$ activates I_{Ca} channels in *Arabidopsis* guard cells mediated by CERK1.

$(GlcNAc)_8$ significantly increased the number of guard cells showing $[Ca^{2+}]_{cyt}$ elevations in wild type ($P < 0.05$), but not in *cerk1-2* ($P = 0.92$) (Fig. 3 *A* and *B*). The amount of Ca^{2+} mobilized in each guard cell showing $[Ca^{2+}]_{cyt}$ elevations was significantly increased by $(GlcNAc)_8$ in wild type but not in *cerk1-2* (Fig. 3*C*). The *cerk1-2* mutation itself did not affect the basal level of Ca^{2+} concentration in guard cells (Fig. 3*D*). These results indicate that $(GlcNAc)_8$ induces $[Ca^{2+}]_{cyt}$ elevation in *Arabidopsis* guard cells in a CERK1-dependent manner.

$(GlcNAc)_8$ Activates SLAC1 Mediated by CERK1 and Ca^{2+} in Guard Cells. Activation of the S-type anion channel is critical for stomatal

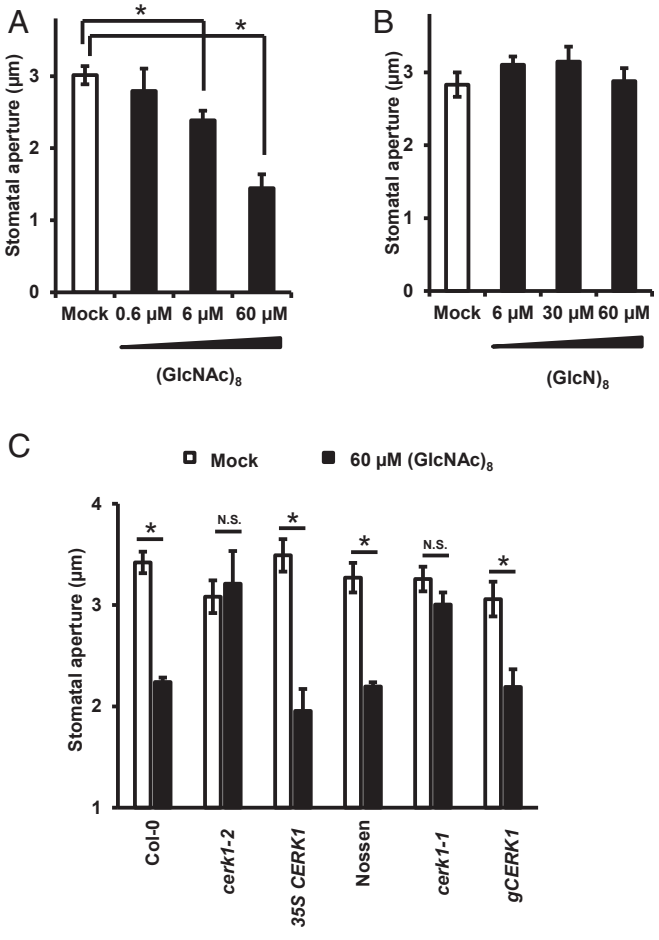

Fig. 1. $(GlcNAc)_8$ but not $(GlcN)_8$ induces stomatal closure mediated by CERK1. (*A* and *B*) Dose effect of $(GlcNAc)_8$ (*A*) and $(GlcN)_8$ (*B*) on Col-0 stomatal aperture. (*C*) $(GlcNAc)_8$-induced stomatal closure in *cerk1* knockout and complemented plants. Averages from three independent experiments (90 total stomata per bar) are shown. Data are mean ± SEM ($n = 3$). Student's *t* test: $^*P < 0.05$; N.S., no significant difference.

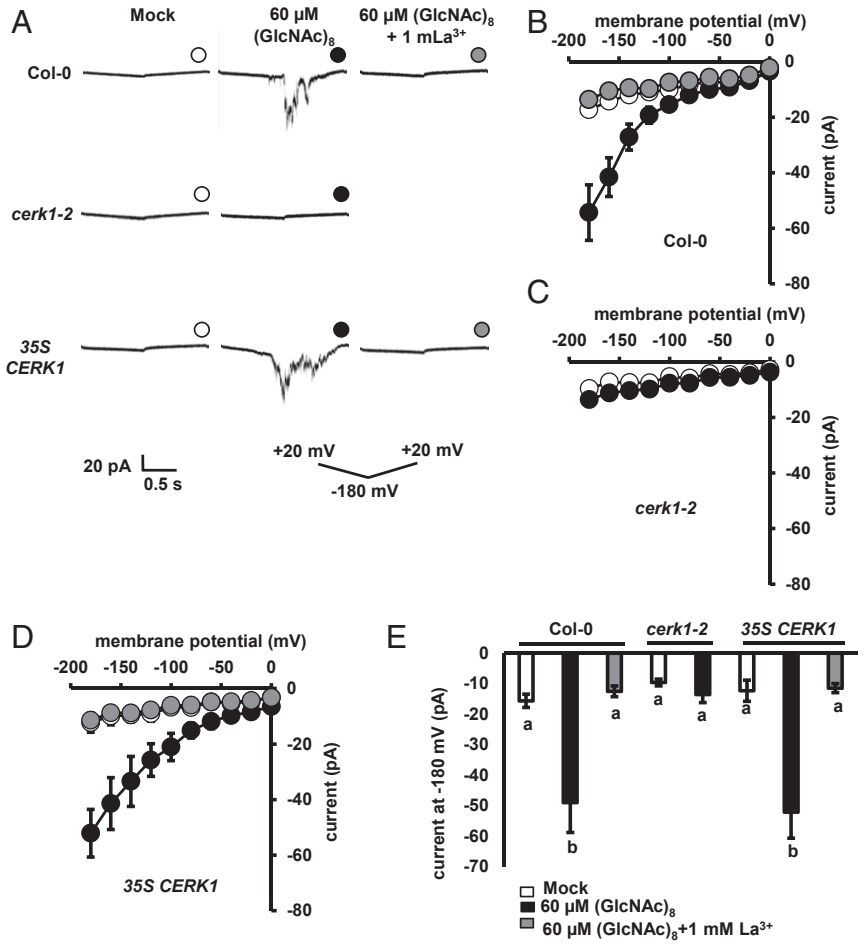

Fig. 2. $(GlcNAc)_8$ activates I_{Ca} channels mediated by CERK1 in guard cells. (*A*) Representative whole-cell I_{Ca} channel current recordings in GCPs. (*B–D*) Average current-voltage curves of whole-cell I_{Ca} channel current recordings in *A*. Data are mean ± SEM ($n = 5$). (*E*) Average currents at −180 mV. Data are mean ± SEM ($n = 5$). Different letters indicate statistical significance ($P < 0.05$, ANOVA with Tukey's test).

closure induced by many kinds of stimuli (25, 26, 28, 42). As shown in Fig. 4, $(GlcNAc)_8$ induced S-type anion channel currents in wild-type GCPs but not in *cerk1-2* when the $[Ca^{2+}]_{cyt}$ was buffered to 2 μM. At the same $[Ca^{2+}]_{cyt}$, *35S CERK1* complemented the defective phenotype of *cerk1-2* GCPs. It is known that elevated $[Ca^{2+}]_{cyt}$ is essential for S-type anion channel activation in response to abiotic stimuli (23, 25). We then investigated the role of Ca^{2+} in $(GlcNAc)_8$-induced S-type anion channel activation. When $[Ca^{2+}]_{cyt}$ was buffered to 150 nM, a basal level of $[Ca^{2+}]_{cyt}$ in guard cells (23, 24, 43), $(GlcNAc)_8$ did not activate S-type anion channel currents (Fig. 4). Taken together, these results indicate that CERK1 and elevated $[Ca^{2+}]_{cyt}$ are essential for $(GlcNAc)_8$ activation of S-type anion channels in *Arabidopsis* guard cells.

The main S-type anion channel in guard cells, SLOW ANION CHANNEL-ASSOCIATED 1 (SLAC1), is crucial for stomatal closure and S-type anion channel activation (44, 45). Recent studies show that Ser59 and Ser120 in SLAC1 can be phosphorylated by CPK6 and OST1 in vitro, and their phosphorylation is critical for ABA-induced stomatal closure and activation of S-type anion channels (27, 29, 46). Here, we investigated the role of SLAC1 and its phosphorylation in $(GlcNAc)_8$ guard cell signaling. $(GlcNAc)_8$-induced stomatal closure and activation of S-type anion channels were impaired by the loss-of-function mutation, *slac1-1* (Fig. 5 *A–D*). In the *slac1-1* complemented plants (established in ref. 29), $(GlcNAc)_8$-induced stomatal closure was complemented by the expression of wild-type SLAC1, SLAC1-WT, and serine-to-alanine mutants, SLAC1-S59A and SLAC1-S120A, but not by SLAC1-S59A S120A double mutant ($P < 0.01$ compared to SLAC1-WT) (Fig. 5*A*). $(GlcNAc)_8$ activation of S-type anion channels was also impaired in the SLAC1-S59A S120A mutant (Fig. 5 *B–D*). Furthermore, loss-of-function mutations of *CPK6* and *OST1* impaired $(GlcNAc)_8$-induced stomatal closure (Fig. 5*E*). These results indicate that SLAC1 and its phosphorylation at Ser59 and Ser120 are required for $(GlcNAc)_8$-induced stomatal closure and activation of S-type anion channels.

To further understand how the CERK1-mediated pathway triggers the activation of SLAC1, the interaction between CERK1 and CPK6, OST1, and SLAC1 was investigated by bimolecular fluorescence complementation (BiFC) and Gal4-based yeast two-hybrid assays. As transient expression of wild-type CERK1 induced cell death in *Nicotiana benthamiana* (38), kinase-dead $CERK1^{D441V}$ was used in the BiFC assay. Clear fluorescent signals were observed with the combination of $CERK1^{D441V}$ plus OST1 and $CERK1^{D441V}$ plus CPK6, but not $CERK1^{D441V}$ plus SLAC1 (Fig. 6*A* and *SI Appendix*, Fig. S4*A*). Note that fluorescence signals were observed when expressing OST1 plus SLAC1, indicating SLAC1 is properly expressed (*SI Appendix*, Fig. S4*A*). To check the specificity of CERK1 interaction signals, we investigated the interaction of CPK6 and OST1 with LYK4, LYK5, and FLAGELLIN-SENSITIVE2 (FLS2), a receptor of bacterial flagellin. YFP signals were observed from LYK4 plus CPK6, LYK5 plus CPK6, FLS2 plus CPK6, LYK4 plus OST1, and LYK5 plus OST1, but not from FLS2 plus

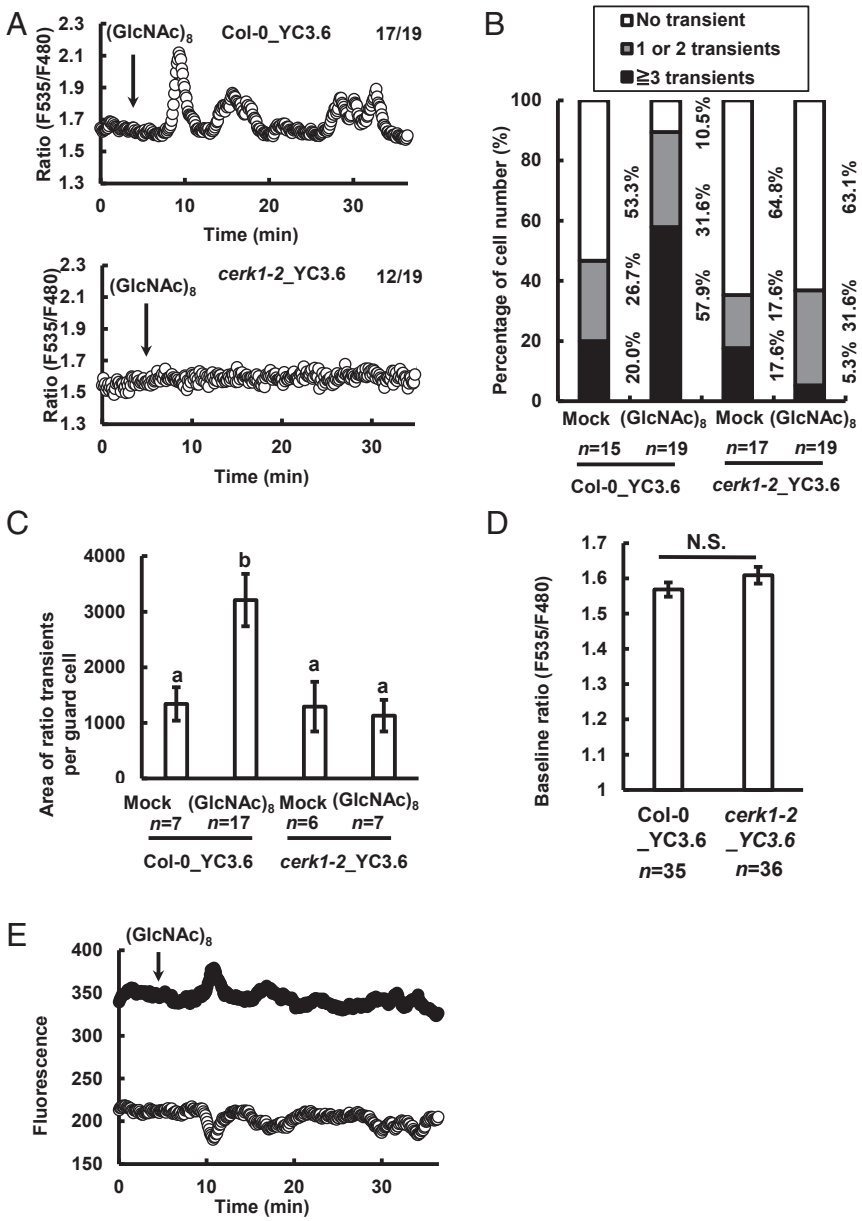

Fig. 3. $(GlcNAc)_8$ induces $[Ca^{2+}]_{cyt}$ elevations in guard cells in a CERK1-dependent manner. (*A*) Representative traces of fluorescence emission ratios (535/480 nm) showing transient $[Ca^{2+}]_{cyt}$ elevations in Col-0 and *cerk1-2* guard cells treated with 60 μM $(GlcNAc)_8$. (*B*) Percentage of number of guard cells showing different number of transient $[Ca^{2+}]_{cyt}$ elevations. (*C*) Area of transients of ratio (F535/F480) elevation in each guard cell showing $[Ca^{2+}]_{cyt}$ elevations in *B*. Area of ratio transients per guard cell was calculated as the sum of areas of ratio transients above the baseline ratio in each guard cell and is considered proportional to the amount of Ca^{2+} mobilized. (*D*) Baseline ratio (F535/F480) in guard cells. (*E*) Traces of fluorescence emission in Col-0 guard cells treated with 60 μM $(GlcNAc)_8$ in *A*. Note that fluorescence at 485 nm (white circles) decreases while fluorescence at 530 nm (black circles) increases, confirming fluorescence resonance energy transfer of the YC3.6 reporter. $(GlcNAc)_8$ was added 5 min after the start of imaging. The average fluorescence ratio in the first 5 min of imaging was considered as the baseline ratio in *D*. $[Ca^{2+}]_{cyt}$ elevations were counted when changes in fluorescence ratios were more than or equal to 0.1 U from the baseline ratio. Data are mean ± SEM. Different letters indicate statistical significance ($P < 0.05$, ANOVA with Tukey's test). N.S., not significant.

OST1 (*SI Appendix*, Fig. S4*A*), suggesting that the interaction with OST1 is specific to CERK1 and its homologs.

Yeast two-hybrid assays detected the interaction of the CERK1 kinase domain with OST1 (Fig. 6*B*) but not with CPK6, SLAC1 N terminus, or SLAC1 C terminus (Fig. 6*B* and *SI Appendix*, Fig. S4*B*). However, under our experimental conditions, the interaction of OST1 and CPK6 with SLAC1 N terminus or C terminus was not detected (*SI Appendix*, Fig. S4*B*), which is not consistent with the previous reports showing phosphorylation of SLAC1 N terminus and C terminus by OST1 and CPK6 in vitro kinase assays (27, 46). The discrepancy could be due to the transient nature of these interactions, which are easier to happen in an in vitro kinase assay with enough amounts of interacting proteins. Based on the above interaction results, we hypothesize that CERK1 interacts with OST1 but not SLAC1 in guard cells while CPK6 is mainly regulated by CERK1-dependent $[Ca^{2+}]_{cyt}$ elevation. These results also led us to test whether $(GlcNAc)_8$ induces OST1 kinase activity. In our in-gel kinase assay, ABA but not $(GlcNAc)_8$ increased OST1 kinase activity (*SI Appendix*, Fig. S5), which suggests that $(GlcNAc)_8$ does not increase OST1 kinase activity in guard cells. Further research is undergoing to investigate how OST1 is involved in $(GlcNAc)_8$ signaling.

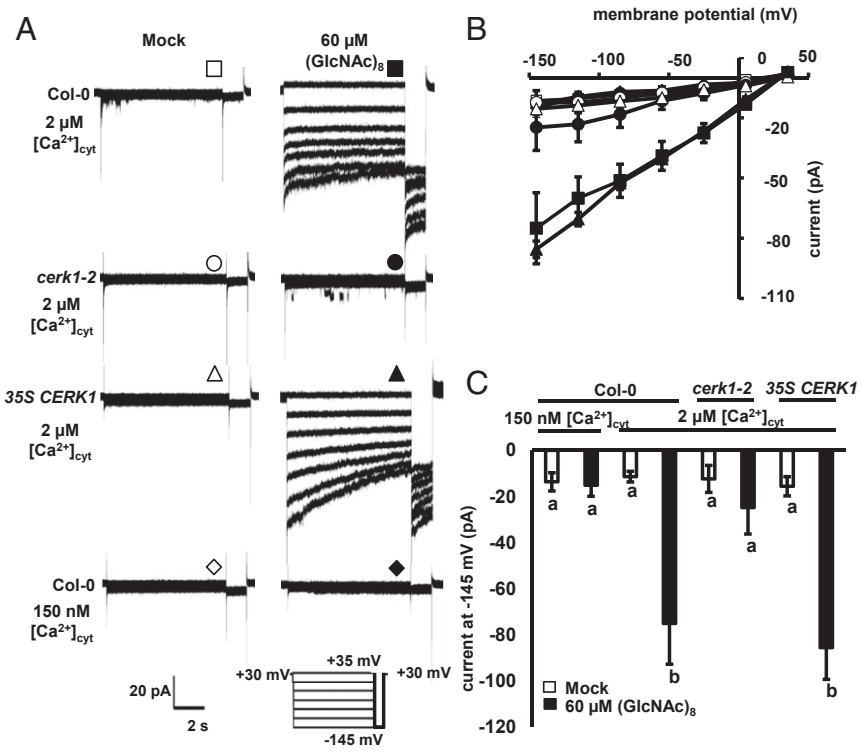

Fig. 4. $(GlcNAc)_8$ activates S-type anion channels mediated by CERK1 and Ca^{2+} in guard cells. (*A*) Representative whole-cell S-type anion channel current recordings in GCPs. (*B*) Average steady-state current-voltage curves of whole-cell S-type anion channel current recordings in *A*. Data are mean ± SEM ($n = 5$). (*C*) Average steady-state S-type anion channel currents at −145 mV. Data are mean ± SEM ($n = 5$). Different letters indicate statistical significance ($P < 0.05$, ANOVA with Tukey's test).

Activation of SLAC1 by CPK6 and OST1 is tightly regulated by not only ABA but also type 2C protein phosphatases such as ABI1 and ABI2 and the ABA receptors PYR/PYL/RCAR (47). Here, to understand where $(GlcNAc)_8$ signaling interacts with ABA signaling, we investigated $(GlcNAc)_8$-dependent stomatal closure in dominant negative mutants in ABA signaling, *abi1-1C* and *abi2-1C*. It was found that $(GlcNAc)_8$-induced stomatal closures were inhibited in the *abi1-1C* and *abi2-1C* (*SI Appendix*, Fig. S3*F*), suggesting that signaling of $(GlcNAc)_8$ and ABA interacts also at the points of type 2C protein phosphatases.

$(GlcN)_8$ Induces Guard Cell Death in a Manner Dependent on Ca^{2+} but Not CERK1. The effects of $(GlcN)_8$ and $(GlcNAc)_8$ on guard cell viability were investigated by fluorescein diacetate (FDA) staining. Mock and CTOS treatment did not significantly affect the FDA staining rates of guard cells (Fig. 7*A*). Unexpectedly, $(GlcN)_8$ treatment significantly decreased the FDA staining rate in a dose-dependent manner with an EC_{50} of 57.87 μM (Fig. 7*A* and *SI Appendix*, Fig. S1*B*) Time-course experiments further show that 60 μM $(GlcN)_8$ massively decreased FDA staining rate after 30 min (*SI Appendix*, Fig. S6*A*). The guard cells treated with $(GlcN)_8$ were also stained by propidium iodide (PI), a fluorescent dye that cannot permeate an intact cellular membrane (*SI Appendix*, Fig. S6 *B–D*). These results indicate that $(GlcN)_8$ induces guard cell death in *Arabidopsis*. $(GlcN)_8$ induced guard cell death also in *cerk1-2, lyk4*, and *lyk5* (Fig. 7*B* and *SI Appendix*, Fig. S7*A*), indicating that CERK1, LYK4, and LYK5 are not essential for the guard cell death.

ROS and Ca^{2+} are known to be involved in cell death induced by many stimuli (34, 35, 48). We performed pharmacological studies to study the roles of ROS and Ca^{2+} in $(GlcN)_8$-induced guard cell death using salicylhydroxamic acid (SHAM) and diphenyleneiodonium (DPI), inhibitors of two major ROS-producing enzymes in guard cells, class III peroxidases and NAD(P)H oxidases (20, 49), and La^{3+}, a broad Ca^{2+} channel blocker. Only La^{3+} treatment but not SHAM or DPI impaired $(GlcN)_8$-induced guard cell death (Fig. 7*C* and *SI Appendix*, Fig. S7 *B* and *C*). Note that $(GlcN)_8$ induced ROS accumulation in guard cells, which is mediated by the enzymes sensitive to SHAM but not to DPI (*SI Appendix*, Fig. S7*D*). $(GlcN)_8$ induced guard cell death in *rbohD rbohF*, a mutant functionally defective in two major NAD(P)H oxidases in guard cells (*SI Appendix*, Fig. S7*A*). These results together suggest that Ca^{2+} but not ROS production is required for $(GlcN)_8$-induced guard cell death in *Arabidopsis*.

We then investigated whether $(GlcN)_8$ activates I_{Ca} channels and induces $[Ca^{2+}]_{cyt}$ elevation in guard cells. $(GlcN)_8$ activated I_{Ca} channel currents in both Col-0 and *cerk1-2* GCPs, which was inhibited by La^{3+} (Fig. 8). Yellow chameleon 3.6-based $[Ca^{2+}]_{cyt}$ imaging shows that $(GlcN)_8$ induced a burst of the fluorescence ratio in both Col-0 and *cerk1-2* guard cells (Fig. 9). However, the CFP fluorescence did not increase back to the basal level while the YFP fluorescence decreased below the basal level, which was in contrast to a proper function of YC3.6 seen in $(GlcNAc)_8$-triggered change of YFP and CYP fluorescence in guard cells (Fig. 3*E*). The malfunction of YC3.6 following the Ca^{2+} burst was also an indicator of the cell death fate. Note that the timing for the Ca^{2+} burst varied from cell to cell, which was consistent with the finding that the timing of cell death varied from cell to cell, as evidenced by some guard cells still alive after 2 h $(GlcN)_8$ treatment (Fig. 7*A*). The lag time needed for the $(GlcN)_8$-induced $[Ca^{2+}]_{cyt}$ elevation suggests that accumulation of signaling intensity or potential transcription and translation events are required for the $[Ca^{2+}]_{cyt}$ elevation.

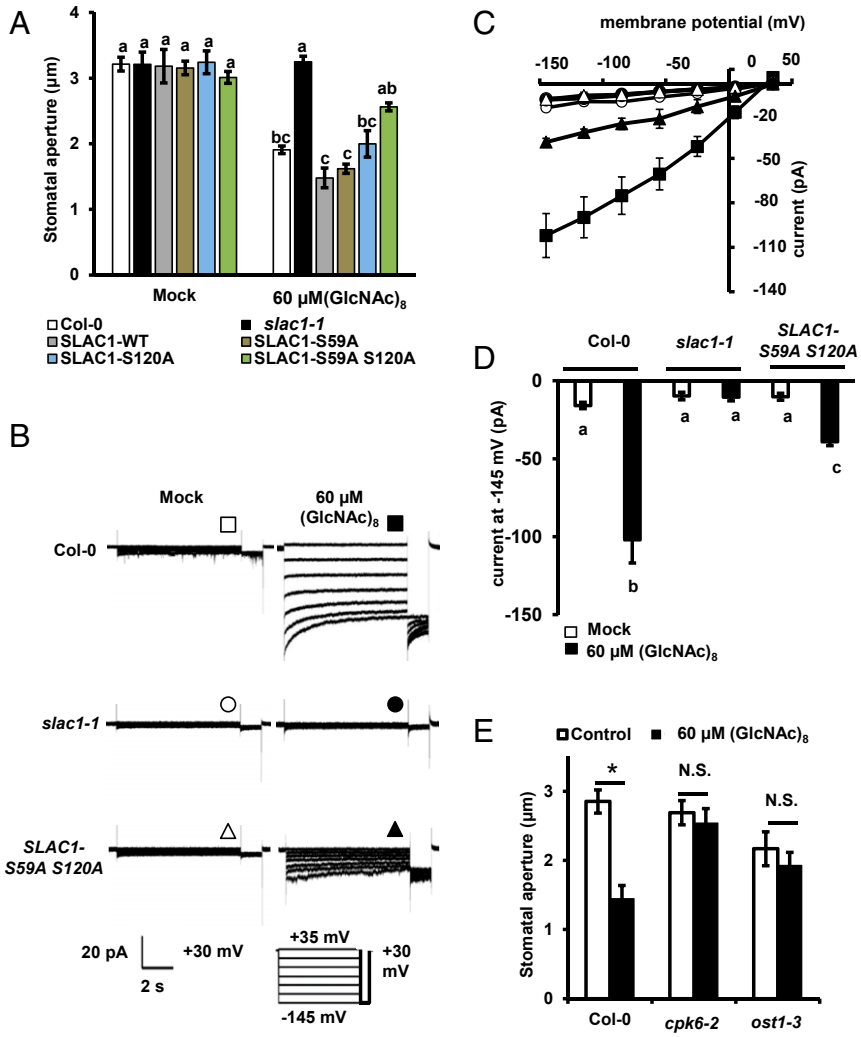

Fig. 5. SLAC1 is required for $(GlcNAc)_8$-induced stomatal closure and activation of S-type anion channels in guard cells. (*A*) $(GlcNAc)_8$-induced stomatal closure in *slac1-1* and complemented lines. Averages from three independent experiments (90 total stomata per bar) are shown. Data are mean ± SEM ($n = 3$). Different letters indicate statistical significance ($P < 0.05$, ANOVA with Tukey's test). (*B*) Representative whole-cell S-type anion channel current recordings in GCPs. (*C*) Average steady-state current-voltage curves of whole-cell S-type anion channel current recordings in *A*. Data are mean ± SEM ($n = 5$). (*D*) Average steady-state S-type anion channel currents at −145 mV. Data are mean ± SEM ($n = 5$). Different letters indicate statistical significance ($P < 0.05$, ANOVA with Tukey's test). (*E*) $(GlcNAc)_8$-induced stomatal closure in Col-0, *cpk6-2*, and *ost1-3*. Averages from three independent experiments (90 total stomata per bar) are shown. Data are mean ± SEM ($n = 3$). Student's *t* test: $^*P < 0.05$. N.S., no significant difference.

Discussion

CTOS as a Model Fungal MAMP to Study Fungus-Induced Stomatal Closure. Several fungal MAMPs have been shown to induce stomatal closure in different plant species, with chitosans of different polymerization and acetylation being the most studied MAMPs (50–52). Studies have suggested that degree of polymerization and acetylation and viscosity are important for chitosan function (53, 54). It is also possible that chitosan functions through CERK1 since partially acetylated chitosan binds to CERK1 (12), and its acetylated moiety could be released by plant chitinases. Nevertheless, because of the heterogenic nature of these chitosans, their mode of function is difficult to be clarified.

To further elucidate fungal MAMP signaling in guard cells, recent studies have begun to investigate the signaling induced by the well-known fungal MAMP, CTOS, in *Arabidopsis*, showing that the 14-3-3 protein is involved in CTOS-induced stomatal closure (55) and that CTOS induces elevation of $[Ca^{2+}]_{cyt}$ (56) and transitions in actin filament organization in guard cells (14). The presented results using synthetic $(GlcNAc)_8$ as a representative CTOS further reveal that CTOS induces stomatal closure through a core signaling mediated by CERK1, I_{Ca} channels, Ca^{2+}, CPK6, PP2Cs, OST1, and SLAC1 in *Arabidopsis*. Given that OST1 and SLAC1 are guard cell-specific genes, it will be interesting to investigate whether their homologs play a role in CTOS signaling in other cell types.

Although OST1 is required for stomatal closure induced by ABA, methyl jasmonate, CO_2, flg22, and fungal MAMPs, its activity is only increased by ABA (31, 57–59) (*SI Appendix*, Fig. S5). Guard cells generally contain much more ABA compared to other cells and have basal OST1 kinase activity under resting conditions (59, 60). Although a model of OST1 function at basal activity in guard cells has been proposed (31, 59), future research is needed to clarify how the basal OST1 activity regulates CTOS signaling and whether interaction with CERK1 plays a role in the regulation.

During the preparation of the manuscript, it was reported that a homolog of SLAC1, SLAH3, but not SLAC1, and a receptor-like cytoplasmic kinase, PBL27, were required for stomatal closure induced by a crude chitin preparation containing long-chain

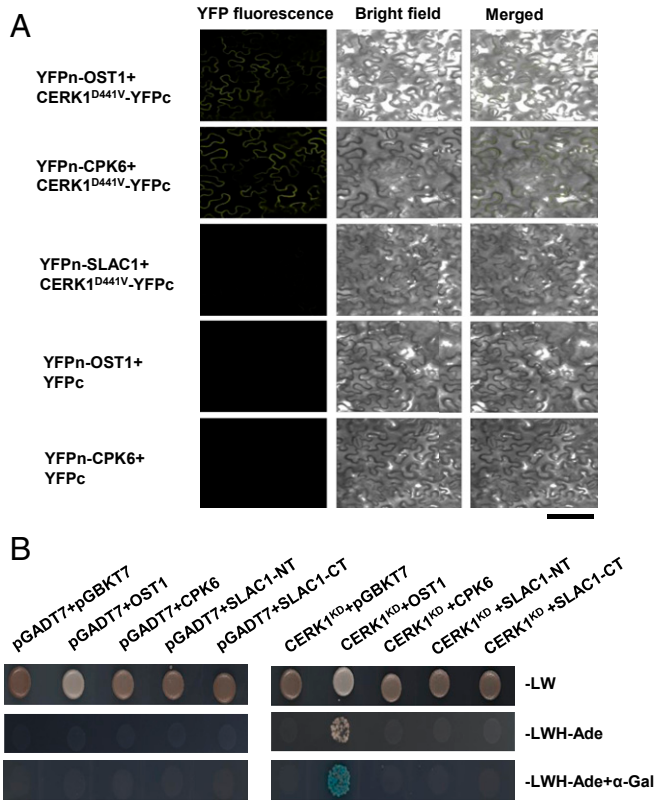

Fig. 6. CERK1 interacts with OST1. (*A*) Confocal microscopy of *N. benthamiana leaves* transiently expressing the indicated split-YFP constructs. Representative images are shown. (Scale bar: 100 μm.) (*B*) Interaction analysis of CERK1 kinase domain ($CERK1^{KD}$) with OST1, CPK6, and SLAC1 N terminus (SLAC1-NT) and C terminus (SLAC1-CT) using yeast two-hybrid assays.

and short-chain CTOS and CSOS at 1 mg/mL (38). On the other hand, the presented results show that SLAH3 and PBL27 are not essential for stomatal closure by a representative CTOS, $(GlcNAc)_8$ (*SI Appendix*, Fig. S3 *D* and *E*). This discrepancy is not fully understood. Probably, it is from the differences in nature of the signaling triggered by mixture and a particular CTOS as seen in previous studies and discussed by Bi and Zhou (61) and by Yamaguchi et al. (62). Studies have shown that interactions between different oligosaccharides play important roles in determining signaling specificity (63). An interesting possibility is that CSOS in the crude chitin preparation may interact with CTOS to define CTOS signaling specificity.

CSOS Induces Guard Cell Death in *Arabidopsis*. Since fully deacetylated forms of CSOS hardly bind to CERK1 and do not induce ROS production in leaf or activation of MAPKs in seedlings in *Arabidopsis* (12, 13), we initially hypothesized that the *Arabidopsis* guard cell does not respond to CSOS. This idea may hold true at low concentration based on our results that $(GlcN)_8$ did not affect stomatal aperture or cell viability at 6 μM, but $(GlcNAc)_8$ induced clear stomatal closure (Figs. 1 and 7). Interestingly, previous studies have observed that wheat rust fungi produce chitin deacetylases and induce a transient stomatal closure in *Arabidopsis* (7, 10). These results together suggest that conversion of CTOS to CSOS by chitin deacetylase is a fungal strategy to evade CTOS-induced stomatal closure.

Surprisingly, CSOS at higher concentrations induces guard cell death, which does not require CERK1 but requires Ca^{2+} influx (Fig. 7). Recent studies have shown that CSOSs induce a series of immune responses to alleviate virus and bacterial infection in *Arabidopsis* (64, 65). These results indicate that *Arabidopsis* cells do perceive CSOS in a CERK1-independent manner. Since CSOS activated I_{Ca} channels in GCPs after the establishment of a whole-cell configuration (Fig. 8), it can be suggested that the sensing of CSOS occurs on the plasma membrane. Studies have found that CSOS binds to several proteins in the plasma membrane (66, 67). It would be interesting to investigate whether these proteins are involved in the CSOS-induced guard cell death. Downstream of Ca^{2+}, Ca^{2+} sensors, including CPKs, are known to be involved in cell death triggered by defense signals (34, 35). Future research is needed to find the Ca^{2+} sensors involved in the CSOS-induced guard cell death.

Guard cell death has been observed in several nonadapted rust fungus–plant interactions and consequently stops the fungal infection through the stomata (7, 68). The results raise the possibility that CSOS sensing triggers the rust fungus-induced guard cell death. Future studies to determine the local concentration of CSOS produced during fungal infection would further shed light on the role of CSOS in the guard cell–fungus interaction. Since CSOS-induced cell death was observed not only in guard cells but also in epidermal cells and mesophyll cells (*SI Appendix*, Fig. S6 *E* and *F*), we speculate that CSOS contributes to the induction of cell death of other plant cell types for resistance against nonadapted fungi. On the other hand, a scenario for necrotrophic fungi is that they may use CSOS in addition to other chemical weapons to kill the host cell for infection. Many pathogenic fungi have strategies to interfere with CTOS-triggered plant immunity. An example is that pathogenic fungi secrete a LysM domain-containing effector, Ecp6, to sequester CTOS but not CSOS from being sensed by plant cells (69). Similarly, it is possible that pathogenic fungi have mechanisms to either avoid or utilize CSOS-triggered cell death for successful infection.

Stomatal Immunity Comprises Not Only Stomatal Closure but Also Guard Cell Death. Plant chitinases, fungal chitin deacetylases, and their hydrolysis products, such as CTOS and CSOS, play important roles in plant–fungus interaction (8, 9). Based on our results, we proposed a model to summarize possible guard cell–fungus interactions (*SI Appendix*, Fig. S8). In the model, CTOS released by plant chitinases induces stomatal closure to prevent fungal invasion. On the other hand, fungi secrete chitin deacetylases to evade stomatal closure. When CSOS accumulates over a threshold, cell death signaling is triggered in guard cells, which eventually prevents most fungal infection. Ca^{2+} as a shared second messenger determines the output of CTOS and CSOS signaling.

Stomatal immunity as part of active plant immunity has been a focus of plant–microbe interaction research in the past decade, which is so far solely understood as stomatal closure induced by microbe invasion (3–5). The presented finding that a guard cell actively executes cell death in response to the conserved fungal cell wall component, CSOS, thus represents a conceptual advance in understanding of stomatal immunity. Given previous observations that bacteria inject a cell death-inducing effector into guard cells to suppress stomatal closure (70, 71), we expect that cell death is a general guard cell defense mechanism, following the failure of stomatal closure, against different pathogens, and believe that the concept that stomatal immunity also includes an active guard cell death would guide future research on guard cell–microbe interaction and crop protection.

In summary, our results suggest that conversion of CTOS to CSOS is a strategy for fungi to facilitate penetration through stomata while guard cells can sense not only CTOS to induce stomatal closure, but also CSOS to induce cell death, eventually warding off most fungal infection.

Materials and Methods

Plant Materials and Growth Conditions. *Arabidopsis* (*Arabidopsis thaliana*) wild type (Columbia), Nossen, *cerk1-2* (40), *35S CERK1* (39), *cerk1-1* (40), *gCERK1*

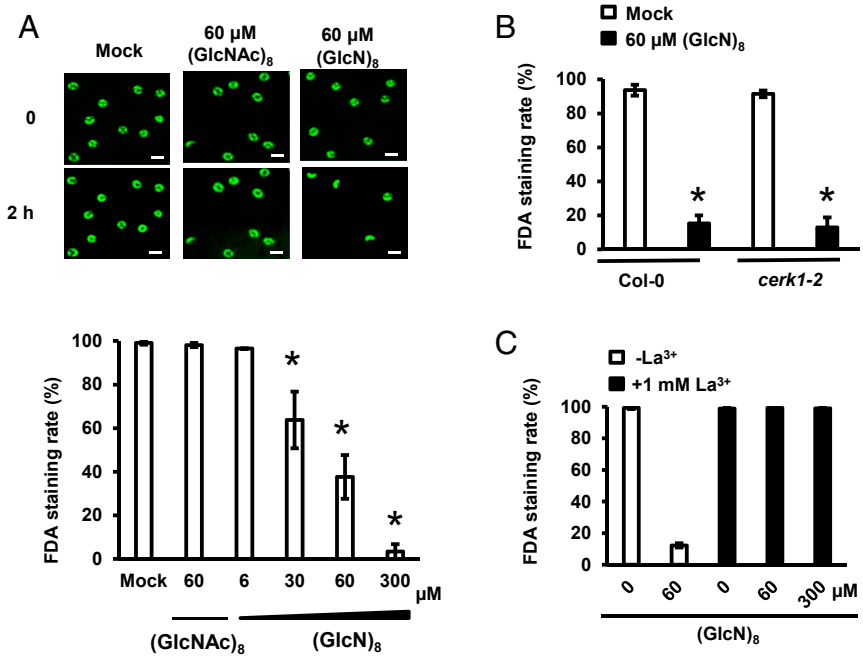

Fig. 7. $(GlcN)_8$ induces guard cell death in a manner dependent on Ca^{2+} but not CERK1. (*A*–*C*) FDA staining rate of guard cells treated with oligosaccharides for 2 h. *A* and *C* are results from Col-0 guard cells. Averages from three independent experiments (100 to 200 guard cells per bar) are shown. Data are mean ± SEM ($n = 3$). Asterisks indicate statistical significance compared to mock treatment in the same genotype ($P < 0.05$, Student's *t* test). (Scale bar: 20 μm.)

(40), *cpk6-2* (28), *ost1-3* (31), *slac1-1* (29), SLAC1-WT (29), SLAC1-S59 (29), SLAC1-S120 (29), SLAC1-S59 S120 (29), *lyk4-2* (72), *lyk5-2* (72), *pbl27-1* (73), *slah3-1* (GK_371G03), *abi1-1C* (31), *abi2-1C* (31), and *rbohD rbohF* (74) were grown in pots filled by a mixture of vermiculite (70% [vol/vol]; Asahi-kogyo, Okayama, Japan) and kureha soil (30% [vol/vol]; Kureha Chemical, Tokyo, Japan) at 22 ± 2 °C with relative humidity of 60 ± 10% in a growth chamber under a 16-h white light (80 $\mu mol \cdot m^{-2} \cdot s^{-1}$)/8-h dark regime. All of the mutants are in the Col-0 ecotype background, except for *cerk1-1*, which is in the Nossen ecotype background. The plants were supplemented with nutrition solution (0.1% Hyponex solution; Hyponex, Osaka, Japan) twice or three times a week. To obtain YC3.6-expressing *cerk1-2* mutants, *cerk1-2* mutants were crossed with wild-type plants expressing YC3.6. Homozygous YC3.6-expressing *cerk1-2* mutants were used for imaging of $[Ca^{2+}]_{cyt}$. For all experiments, the plants used were 4 to 6 wk old.

$(GlcNAc)_8$ and $(GlcN)_8$. $(GlcN)_8$ was kindly provided by Yaizu Suisankagaku Industry Co., Ltd., Shizuoka, Japan. $(GlcNAc)_8$ was prepared by re-N-acetylation of the $(GlcN)_8$ (75). No contaminant such as $(GlcN)_8$ in the prepared $(GlcNAc)_8$ was detected by matrix-assisted laser desorption ionization time-of-flight mass spectroscopy (75). The same $(GlcNAc)_8$ has been used in a series of previous studies (40, 76–78). Stock solutions of $(GlcNAc)_8$ and $(GlcN)_8$ were prepared using water as solvent and diluted to required concentrations in the buffers for each experiment. Mock treatment and oligosaccharide treatment were performed by replacing the preincubation buffers with the same buffers without or with oligosaccharides.

Stomatal Aperture Measurement. Leaf discs (3 mm in diameter) from fully expanded rosette leaves were floated on solution [5 mM KCl, 50 μM $CaCl_2$, and 10 mM 2-(*N*-morpholino)ethanesulfonic acid (MES)-Tris (pH 6.15)] with

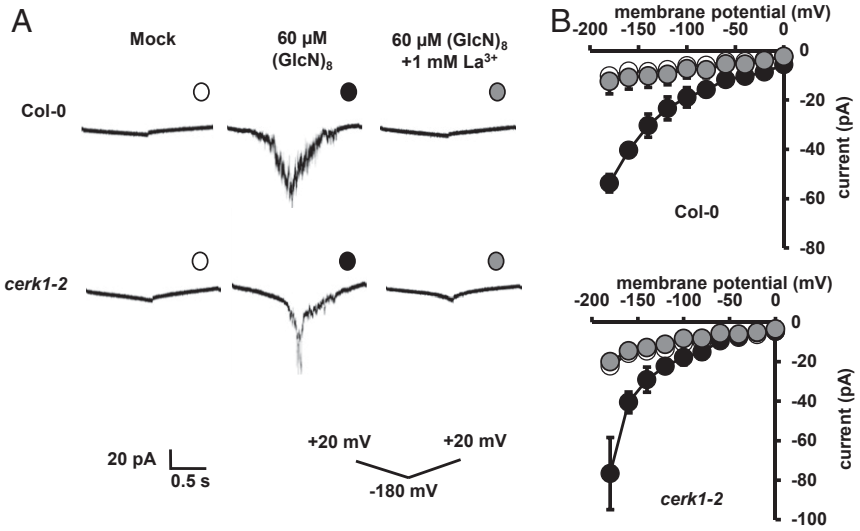

Fig. 8. $(GlcN)_8$ activates I_{Ca} channels in guard cells. (*A*) Representative whole-cell I_{Ca} channel current recordings in GCPs. (*B*) Average current-voltage curves of whole-cell I_{Ca} channel current recordings in *A*. Data are mean ± SEM ($n = 5$ for Col-0; $n = 3$ for *cerk1-2*).

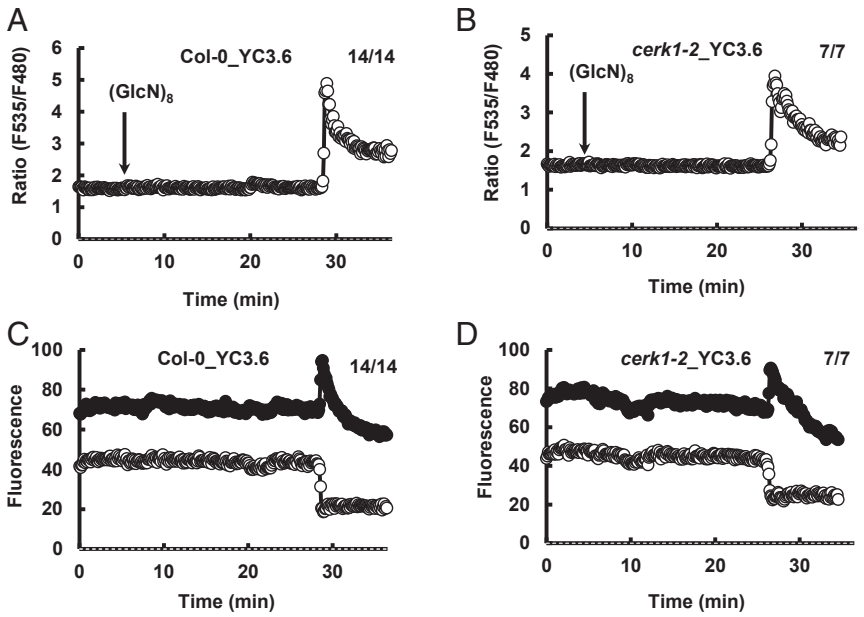

Fig. 9. $(GlcN)_8$ induces $[Ca^{2+}]_{cyt}$ elevations in guard cells. (*A* and *B*) Representative traces of fluorescence emission ratios (535/480 nm) in Col-0 ($n = 14$) and *cerk1-2* guard cells ($n = 7$) treated with 60 μM $(GlcN)_8$. (*C* and *D*) Traces of fluorescence emission (535 nm, black circles; 480 nm, white) in *A* and *B*. Note that all of the guard cells monitored showed similar patterns of change of fluorescence with the timing of ratio burst varying from cell to cell.

their adaxial surface upward in the light for 2 h to create a condition that most of the stomata are open before MAMP treatment. Then $(GlcNAc)_8$ or $(GlcN)_8$ at the indicated concentration was added, and the leaf discs were incubated in the light for another 2 h before measurement. The stomatal apertures in the abaxial epidermis of leaf discs were imaged using a microscope (Biozero BZ-8000; Keyence, Osaka, Japan), followed by measurement using Image J software (NIH, Bethesda, MD). For each sample, apertures of 30 stomata were measured.

Patch-Clamp Measurement. Measurements of I_{Ca} and S-type anion channel currents in *Arabidopsis* GCPs were performed as described previously (26, 31). For measurement of I_{Ca} channel currents, a whole-cell configuration was established firstly and then was recorded 16 times to get averages for control. After adding 60 μM $(GlcNAc)_8$ extracellularly, the GCPs were recorded for 16 times to get averages for the $(GlcNAc)_8$ treatment. After adding 1 mM La^{3+} in the presence of 60 μM $(GlcNAc)_8$, the GCPs were recorded for 16 times to get averages for the $(GlcNAc)_8$+La^{3+} treatment. The interpulse period was 1 min. For measurement of whole-cell S-type anion channel currents, GCPs were treated with $(GlcNAc)_8$ for 2 h before recordings.

FDA and PI Staining. Rosette leaves were excised and gently mounted on a glass slide with the adaxial side upward using a medical adhesive (Hollister). Then, the adaxial epidermis and the mesophyll tissue were removed by a razor blade leaving lower epidermis intact on the slide. The lower epidermis was submerged in solution (5 mM KCl, 50 μM $CaCl_2$, and 10 mM MES-Tris [pH 6.15]) at 22 °C in the light for 3 h resting. After staining of the epidermis with FDA (2 μg/mL), guard cells were imaged using a fluorescent microscope (Biozero BZ-X700; Keyence, Osaka, Japan) and then treated with oligosaccharides for 2 h, followed by imaging again. Inhibitors were added 30 min before oligosaccharide treatment. Only the guard cells stained by FDA before treatment were taken into account for the calculation of FDA staining rate, which was considered as the ratio of the number of FDA-stained guard cells after treatment to the number before. Propidium iodide at 10 μg/mL was used for staining. For FDA and PI double staining, guard cells were imaged using a fluorescent microscope (Leica DM2500; Leica Microsystems, Wetzlar, Germany)

Mesophyll protoplasts used for FDA staining were prepared according to ref. 79. After treatment of $(GlcN)_8$ for 2 h, mesophyll protoplasts were subjected to FDA staining.

Imaging of $[Ca^{2+}]_{cyt}$ in Guard Cells. For the measurement of $[Ca^{2+}]_{cyt}$ in guard cells, YC3.6-expressing wild-type and *cerk1-2* plants were used according to our previous methods (28, 31). $(GlcNAc)_8$ and $(GlcN)_8$ were applied 5 min after the start of imaging.

Quantitative RT-PCR. RNA from rosette leaves was extracted using NucleoSpin RNA Plant (Takara). Then, 500 ng of RNA was used to synthesize cDNA using PrimeScript RT Master Mix (Perfect Real Time) (TaKaRa Bio). Quantitative PCR was performed using Power SYBR Green PCR Master Mix and a StepOne Real-Time PCR System (Applied Biosystems, Carlsbad, CA). Primers used in PCR amplification are as follows: 5′-GGAGAAGTGTCTGCAAAAGTAG-3′ and 5′-CTACCGGCCGGACATAAGACTG-3′ for *CERK1*; and 5′-TGCGCTGCCAGATAA TACACTATT-3′ and 5′-TGCTGCCCAACATCAGGTT-3′ for *UBQ10*.

BiFC Assay. The coding sequences of OST1, LYK4, LYK5, FLS2, CPK6, and SLAC1 were amplified using the primers shown in *SI Appendix*, Table S1 and then cloned into pXY106 to generate YFPn-OST1, LYK4-YFPc, LYK5-YFPc, FLS2-YFPc, YFPn-CPK6, and YFPn-SLAC1. $CERK1^{D441V}$ was amplified by overlap extension PCR using the primer shown in *SI Appendix*, Table S1 and then cloned into pXY104 to produce $CERK1^{D441V}$-YFPc. All constructs were transformed into *Agrobacterium tumefaciens* strain GV3101 for transient expression in *N. benthamiana* by agro-infiltration. Leaves were collected 2 d after infiltration and subjected to confocal microscopy (Leica TCS SP5II) for fluorescence detection.

Yeast Two-Hybrid Assay. A Gal4-based yeast two-hybrid assay was performed as described below. The coding sequence of the CERK1 kinase domain was cloned into the pGADT7 vector in frame with the activation domain using the EcoRI site. The coding sequence of CPK6, OST1, and C terminus and N terminus of SLAC1 were cloned into pGBKT7 in frame with the DNA-binding domain using EcoRI and SalI sites. These vectors were then introduced into the yeast strain Y2H Gold by the lithium acetate method. The transformants were selected on synthetic dropout nutrient medium (SD-Leu/-Trp). Positive colonies were transferred to selective mediums (SD-Leu/-Trp/-His/-Ade) and (SD-Leu/-Trp/-His/-Ade/+X-α-Gal) for verification of interacting proteins. The primers used for amplifying the coding sequences are shown in *SI Appendix*, Table S1.

Quantification of ROS Accumulated in Guard Cells. ROS accumulation in guard cells was evaluated using 2′,7′-dichlorodihydrofluorescein diacetate (H2DCF-DA) according to our previous method (28). Epidermal tissues were treated with 60 μM $(GlcN)_8$ for 15 min to induce ROS accumulation in guard cells.

Water Loss of Detached Leaves. Detached fully expanded rosette leaves were floated on solution (5 mM KCl, 50 μM $CaCl_2$, and 10 mM MES-Tris [pH 6.15]) with their petioles immersed and adaxial surface upward in the light for 2 h. Then, 60 μM $(GlcNAc)_8$ and 10 μM ABA were added, and the leaves were kept in the light for another 1 h. After surface drying, the fresh weight was

determined at indicated time points up to 2 h. Relative water loss was represented by the weight of the leaves at various time points divided by the original weight.

In-Gel Kinase Assay. Ten- to 14-d-old seedlings were treated with 10 μM ABA and 60 μM $(GlcNAc)_8$ for 30 min and then flash frozen in liquid nitrogen for protein extraction. An in-gel kinase assay using protein extracted from the seedlings was performed as described previously (29). The radioactivity of the gel was visualized using Imaging Plate BAS-IP MS 2325 (FUJIFILM, Tokyo, Japan) and BAS imaging analyzer FLA-7000 (FUJIFILM).

Statistical Analysis. Student's *t* test and ANOVA with Tukey's test were used to assess the significance of differences between datasets. The response of $[Ca^{2+}]_{cyt}$ was assessed by χ^2 test. Differences were considered significant for $P < 0.05$.

Accession Numbers. *Arabidopsis* Genome Initiative numbers for the genes discussed in this article are as follows: *ABI1* (AT4G26080), *ABI2* (AT5G57050), *CERK1* (AT3G21630), *CPK6* (AT2G17290), *FLS2* (AT5G46330), *LYK4* (AT2G23770), *LYK5* (AT2G33580), *OST1* (AT4G33950), *PBL27* (AT5G18610), *RBOHD* (AT5G47910), *RBOHF* (AT1G64060), *SLAC1* (At1g12480), and *SLAH3* (AT5G24030).

Data Availability. All study data are included in the article and *SI Appendix*.

ACKNOWLEDGMENTS. We thank Dr. Yoshitake Desaki (Meiji University) for preparing materials; Dr. Julian I. Schroeder (University of California San Diego) for providing seeds of *slac1-1*, SLAC1-WT, SLAC1-S59A, SLAC1-S120A, and SLAC1-S59A S120A; Dr. Takashi Hirayama (Institute of Plant Science and Resources, Okayama University) for providing *abi1-1C* and *abi2-1C* seeds; and Dr. Yuichiro Takahashi (Okayama University) and Dr. Kazuhiro Toyoda (Okayama University) for the use of the BAS imaging analyzer FLA-7000 and imaging plates. This work was supported by the National Natural Science Foundation of China (31901984 to W.Y.); the Start-up Fund from Shanghai Jiao Tong University (WF220515002 to W.Y.); Grants-in-Aid for Japan Society for the Promotion of Science Fellows (267977 and 17F17091 to W.Y.) from the Japan Society for the Promotion of Science, National Key R & D Program of China (100300 to J.L.); the Shanghai Science and Technology Commission (18391900400 to J.L.); the China Agriculture Research System (CARS-29-yc-2 to J.L.); Grants-in-Aid for Scientific Research from the Ministry of Education, Culture, Sports, Science and Technology, Japan (15H05956 to T.K.) and the Advanced Low Carbon Technology Research and Development Program from the Japan Science and Technology Agency (to T.K.); Grants-in-Aid for Scientific Research on Innovative Areas (15H01240 to H.K.); and the Ministry of Education, Culture, Sports, Science and Technology (MEXT)-Supported Program for the Strategic Research Foundation at Private Universities 2014–2018 (S1411023 to H.K.) from the Ministry of Education, Culture, Sports, Science and Technology, Japan.

1. M. Melotto, W. Underwood, S. Y. He, Role of stomata in plant innate immunity and foliar bacterial diseases. *Annu. Rev. Phytopathol.* **46**, 101–122 (2008).
2. M. K. Grimmer, M. John Foulkes, N. D. Paveley, Foliar pathogenesis and plant water relations: A review. *J. Exp. Bot.* **63**, 4321–4331 (2012).
3. D. Arnaud, I. Hwang, A sophisticated network of signaling pathways regulates stomatal defenses to bacterial pathogens. *Mol. Plant* **8**, 566–581 (2015).
4. W. Ye, Y. Murata, Microbe associated molecular pattern signaling in guard cells. *Front. Plant Sci.* **7**, 583 (2016).
5. M. Melotto, L. Zhang, P. R. Oblessuc, S. Y. He, Stomatal defense a decade later. *Plant Physiol.* **174**, 561–571 (2017).
6. J. Zhao, M. Wang, X. Chen, Z. Kang, Role of alternate hosts in epidemiology and pathogen variation of cereal rusts. *Annu. Rev. Phytopathol.* **54**, 207–228 (2016).
7. R. Shafiei, C. Hang, J. G. Kang, G. J. Loake, Identification of loci controlling non-host disease resistance in Arabidopsis against the leaf rust pathogen Puccinia triticina. *Mol. Plant Pathol.* **8**, 773–784 (2007).
8. A. Sánchez-Vallet, J. R. Mesters, B. P. H. J. Thomma, P. de Wit, The battle for chitin recognition in plant-microbe interactions. *FEMS Microbiol. Rev.* **39**, 171–183 (2015).
9. T. Shinya, T. Nakagawa, H. Kaku, N. Shibuya, Chitin-mediated plant-fungal interactions: Catching, hiding and handshaking. *Curr. Opin. Plant Biol.* **26**, 64–71 (2015).
10. N. E. El Gueddari, U. Rauchhaus, B. M. Moerschbacher, H. B. Deising, Developmentally regulated conversion of surface-exposed chitin to chitosan in cell walls of plant pathogenic fungi. *New Phytol.* **156**, 103–112 (2002).
11. S. Cord-Landwehr, R. L. Melcher, S. Kolkenbrock, B. M. Moerschbacher, A chitin deacetylase from the endophytic fungus Pestalotiopsis sp. efficiently inactivates the elicitor activity of chitin oligomers in rice cells. *Sci. Rep.* **6**, 38018 (2016).
12. E. K. Petutschnig, A. M. E. Jones, L. Serazetdinova, U. Lipka, V. Lipka, The lysin motif receptor-like kinase (LysM-RLK) CERK1 is a major chitin-binding protein in Arabidopsis thaliana and subject to chitin-induced phosphorylation. *J. Biol. Chem.* **285**, 28902–28911 (2010).
13. E. Gubaeva *et al*., "Slipped sandwich" model for chitin and chitosan perception in arabidopsis. *Mol. Plant Microbe Interact.* **31**, 1145–1153 (2018).
14. M. Shimono *et al*., Quantitative evaluation of stomatal cytoskeletal patterns during the activation of immune signaling in Arabidopsis thaliana. *PLoS One* **11**, e0159291 (2016).
15. K. Mendgen, M. Hahn, H. Deising, Morphogenesis and mechanisms of penetration by plant pathogenic fungi. *Annu. Rev. Phytopathol.* **34**, 367–386 (1996).
16. K. Shimazaki, M. Doi, S. M. Assmann, T. Kinoshita, Light regulation of stomatal movement. *Annu. Rev. Plant Biol.* **58**, 219–247 (2007).
17. K. E. Hubbard, R. S. Siegel, G. Valerio, B. Brandt, J. I. Schroeder, Abscisic acid and CO_2 signalling via calcium sensitivity priming in guard cells, new CDPK mutant phenotypes and a method for improved resolution of stomatal stimulus-response analyses. *Ann. Bot.* **109**, 5–17 (2012).
18. Y. Murata, I. C. Mori, S. Munemasa, Diverse stomatal signaling and the signal integration mechanism. *Annu. Rev. Plant Biol.* **66**, 369–392 (2015).
19. D. W. A. Hamilton, A. Hills, B. Kohler, M. R. Blatt, Ca^{2+} channels at the plasma membrane of stomatal guard cells are activated by hyperpolarization and abscisic acid. *Proc. Natl. Acad. Sci. U.S.A.* **97**, 4967–4972 (2000).
20. Z. M. Pei *et al*., Calcium channels activated by hydrogen peroxide mediate abscisic acid signalling in guard cells. *Nature* **406**, 731–734 (2000).
21. D. W. A. Hamilton, A. Hills, M. R. Blatt, Extracellular Ba^{2+} and voltage interact to gate Ca2+ channels at the plasma membrane of stomatal guard cells. *FEBS Lett.* **491**, 99–103 (2001).
22. Y. Wang, Z. H. Chen, B. Zhang, A. Hills, M. R. Blatt, PYR/PYL/RCAR abscisic acid receptors regulate K^+ and Cl^- channels through reactive oxygen species-mediated activation of Ca^{2+} channels at the plasma membrane of intact Arabidopsis guard cells. *Plant Physiol.* **163**, 566–577 (2013).
23. R. S. Siegel *et al*., Calcium elevation-dependent and attenuated resting calcium-dependent abscisic acid induction of stomatal closure and abscisic acid-induced enhancement of calcium sensitivities of S-type anion and inward-rectifying K channels in Arabidopsis guard cells. *Plant J.* **59**, 207–220 (2009).
24. Z. H. Chen, A. Hills, C. K. Lim, M. R. Blatt, Dynamic regulation of guard cell anion channels by cytosolic free Ca2+ concentration and protein phosphorylation. *Plant J.* **61**, 816–825 (2010).
25. S. Xue *et al*., Central functions of bicarbonate in S-type anion channel activation and OST1 protein kinase in CO_2 signal transduction in guard cell. *EMBO J.* **30**, 1645–1658 (2011).
26. I. C. Mori *et al*., CDPKs CPK6 and CPK3 function in ABA regulation of guard cell S-type anion- and $Ca^{(2+)}$-permeable channels and stomatal closure. *PLoS Biol.* **4**, e327 (2006).
27. D. Geiger *et al*., Activity of guard cell anion channel SLAC1 is controlled by drought-stress signaling kinase-phosphatase pair. *Proc. Natl. Acad. Sci. U.S.A.* **106**, 21425–21430 (2009).
28. W. Ye *et al*., Calcium-dependent protein kinase CPK6 positively functions in induction by yeast elicitor of stomatal closure and inhibition by yeast elicitor of light-induced stomatal opening in Arabidopsis. *Plant Physiol.* **163**, 591–599 (2013).
29. B. Brandt *et al*., Calcium specificity signaling mechanisms in abscisic acid signal transduction in Arabidopsis guard cells. *eLife* **4**, e3599 (2015).
30. A. Guzel Deger *et al*., Guard cell SLAC1-type anion channels mediate flagellin-induced stomatal closure. *New Phytol.* **208**, 162–173 (2015).
31. W. Ye *et al*., Open stomata 1 kinase is essential for yeast elicitor-induced stomatal closure in arabidopsis. *Plant Cell Physiol.* **56**, 1239–1248 (2015).
32. E. Merilo *et al*., Stomatal VPD response: There is more to the story than ABA. *Plant Physiol.* **176**, 851–864 (2018).
33. F. Pantin, M. R. Blatt, Stomatal response to humidity: Blurring the boundary between active and passive movement. *Plant Physiol.* **176**, 485–488 (2018).
34. R. Ali *et al*., Death don't have no mercy and neither does calcium: Arabidopsis CYCLIC NUCLEOTIDE GATED CHANNEL2 and innate immunity. *Plant Cell* **19**, 1081–1095 (2007).
35. X. Gao *et al*., Bifurcation of Arabidopsis NLR immune signaling via Ca^{2+}-dependent protein kinases. *PLoS Pathog.* **9**, e1003127 (2013).
36. T. Liu *et al*., Chitin-induced dimerization activates a plant immune receptor. *Science* **336**, 1160–1164 (2012).
37. Y. Cao *et al*., The kinase LYK5 is a major chitin receptor in Arabidopsis and forms a chitin-induced complex with related kinase CERK1. *eLife* **3**, e3766 (2014).
38. Y. Liu *et al*., Anion channel SLAH3 is a regulatory target of chitin receptor-associated kinase PBL27 in microbial stomatal closure. *eLife* **8**, e44474 (2019).
39. M. Suzuki *et al*., Autophosphorylation of specific threonine and tyrosine residues in arabidopsis CERK1 is essential for the activation of chitin-induced immune signaling. *Plant Cell Physiol.* **57**, 2312–2322 (2016).
40. A. Miya *et al*., CERK1, a LysM receptor kinase, is essential for chitin elicitor signaling in Arabidopsis. *Proc. Natl. Acad. Sci. U.S.A.* **104**, 19613–19618 (2007).
41. M. Jezek, M. R. Blatt, The membrane transport system of the guard cell and its integration for stomatal dynamics. *Plant Physiol.* **174**, 487–519 (2017).
42. D. Hua *et al*., A plasma membrane receptor kinase, GHR1, mediates abscisic acid- and hydrogen peroxide-regulated stomatal movement in Arabidopsis. *Plant Cell* **24**, 2546–2561 (2012).
43. A. Grabov, M. R. Blatt, Membrane voltage initiates Ca2+ waves and potentiates Ca2+ increases with abscisic acid in stomatal guard cells. *Proc. Natl. Acad. Sci. U.S.A.* **95**, 4778–4783 (1998).
44. J. Negi *et al*., CO_2 regulator SLAC1 and its homologues are essential for anion homeostasis in plant cells. *Nature* **452**, 483–486 (2008).
45. T. Vahisalu *et al*., SLAC1 is required for plant guard cell S-type anion channel function in stomatal signalling. *Nature* **452**, 487–491 (2008).

46. B. Brandt *et al*., Reconstitution of abscisic acid activation of SLAC1 anion channel by CPK6 and OST1 kinases and branched ABI1 PP2C phosphatase action. *Proc. Natl. Acad. Sci. U.S.A.* **109**, 10593–10598 (2012).
47. S. Munemasa *et al*., Mechanisms of abscisic acid-mediated control of stomatal aperture. *Curr. Opin. Plant Biol.* **28**, 154–162 (2015).
48. R. Mittler, ROS are good. *Trends Plant Sci.* **22**, 11–19 (2017).
49. A. R. Khokon *et al*., Involvement of extracellular oxidative burst in salicylic acid-induced stomatal closure in Arabidopsis. *Plant Cell Environ.* **34**, 434–443 (2011).
50. N. Srivastava, V. K. Gonugunta, M. R. Puli, A. S. Raghavendra, Nitric oxide production occurs downstream of reactive oxygen species in guard cells during stomatal closure induced by chitosan in abaxial epidermis of Pisum sativum. *Planta* **229**, 757–765 (2009).
51. S. Koers, A. Guzel-Deger, I. Marten, M. R. G. Roelfsema, Barley mildew and its elicitor chitosan promote closed stomata by stimulating guard-cell S-type anion channels. *Plant J.* **68**, 670–680 (2011).
52. M. A. Salam *et al*., MAP kinases, MPK9 and MPK12, regulate chitosan-induced stomatal closure. *Biosci. Biotechnol. Biochem.* **76**, 1785–1787 (2012).
53. H. Kauss, W. Jeblick, A. Domard, The degrees of polymerization and N-acetylation of chitosan determine its ability to elicit callose formation in suspension cells and protoplasts of Catharanthus roseus. *Planta* **178**, 385–392 (1989).
54. M. Iriti, F. Faoro, Chitosan as a MAMP, searching for a PRR. *Plant Signal. Behav.* **4**, 66–68 (2009).
55. R. Lozano-Durán, G. Bourdais, S. Y. He, S. Robatzek, The bacterial effector HopM1 suppresses PAMP-triggered oxidative burst and stomatal immunity. *New Phytol.* **202**, 259–269 (2014).
56. N. F. Keinath *et al*., Live cell imaging with R-GECO1 sheds light on flg22- and chitin-induced transient $[Ca^{(2+)}]_{cyt}$ patterns in arabidopsis. *Mol. Plant* **8**, 1188–1200 (2015).
57. J. L. Montillet *et al*., An abscisic acid-independent oxylipin pathway controls stomatal closure and immune defense in Arabidopsis. *PLoS Biol.* **11**, e1001513 (2013).
58. Y. Yin *et al*., Involvement of OST1 protein kinase and PYR/PYL/RCAR receptors in methyl jasmonate-induced stomatal closure in arabidopsis guard cells. *Plant Cell Physiol.* **57**, 1779–1790 (2016).
59. L. Zhang *et al*., FRET kinase sensor development reveals SnRK2/OST1 activation by ABA but not by MeJA and high CO_2 during stomatal closure. *eLife* **9**, e56351 (2020).
60. R. Waadt *et al*., FRET-based reporters for the direct visualization of abscisic acid concentration changes and distribution in Arabidopsis. *eLife* **3**, e01739 (2014).
61. G. Bi, J. Zhou, Future studies are needed to determine specificity of PBL27 and MAPKKK5 in immune signaling. Plant Cell supplemental comment (2019). www.plantcell.org/content/plantcell/suppl/2019/09/24/tpc.17.00981.DC2/TPC17.00981Reply.pdf. Accessed 24 September 2019.
62. K. Yamaguchi *et al*, Variable dependencies of PBL27 and MAPKKK5 in chitin-induced MAPK activation in Arabidopsis: Types of chitin and plant growth conditions matter. Plant Cell supplemental comment (2019). www.plantcell.org/content/plantcell/suppl/2019/09/24/tpc.17.00981.DC2/TPC17.00981Comment.pdf. Accessed 24 September 2019.
63. F. Feng *et al*., A combination of chitooligosaccharide and lipochitooligosaccharide recognition promotes arbuscular mycorrhizal associations in Medicago truncatula. *Nat. Commun.* **10**, 5047 (2019).
64. X. Jia, Q. Meng, H. Zeng, W. Wang, H. Yin, Chitosan oligosaccharide induces resistance to Tobacco mosaic virus in Arabidopsis via the salicylic acid-mediated signalling pathway. *Sci. Rep.* **6**, 26144 (2016).
65. X. Jia, H. Zeng, W. Wang, F. Zhang, H. Yin, Chitosan oligosaccharide induces resistance to Pseudomonas syringae pv. tomato DC3000 in Arabidopsis thaliana by activating both salicylic acid- and jasmonic acid-mediated pathways. *Mol. Plant Microbe Interact.* **31**, 1271–1279 (2018).
66. H. Chen, L. Xu, Isolation and characterization of a novel chitosan-binding protein from non-heading Chinese cabbage leaves. *J. Integr. Plant Biol.* **47**, 452–456 (2005).
67. D. Liu *et al*., Identification of chitosan oligosaccharides binding proteins from the plasma membrane of wheat leaf cell. *Int. J. Biol. Macromol.* **111**, 1083–1090 (2018).
68. U. S. Gill, S. R. Uppalapati, J. Nakashima, K. S. Mysore, Characterization of Brachypodium distachyon as a nonhost model against switchgrass rust pathogen Puccinia emaculata. *BMC Plant Biol.* **15**, 113 (2015).
69. R. de Jonge *et al*., Conserved fungal LysM effector Ecp6 prevents chitin-triggered immunity in plants. *Science* **329**, 953–955 (2010).
70. D. Lee, G. Bourdais, G. Yu, S. Robatzek, G. Coaker, Phosphorylation of the plant immune regulator RPM1-INTERACTING PROTEIN4 enhances plant plasma membrane H^+-ATPase activity and inhibits flagellin-triggered immune responses in arabidopsis. *Plant Cell* **27**, 2042–2056 (2015).
71. Z. Zhou *et al*., An arabidopsis plasma membrane proton ATPase modulates JA signaling and is exploited by the Pseudomonas syringae effector protein AvrB for stomatal invasion. *Plant Cell* **27**, 2032–2041 (2015).
72. Y. Desaki *et al*., OsCERK1 plays a crucial role in the lipopolysaccharide-induced immune response of rice. *New Phytol.* **217**, 1042–1049 (2018).
73. T. Shinya *et al*., Selective regulation of the chitin-induced defense response by the Arabidopsis receptor-like cytoplasmic kinase PBL27. *Plant J.* **79**, 56–66 (2014).
74. M. M. Islam *et al*., Reactive carbonyl species function as signal mediators downstream of H_2O_2 production and regulate $[Ca^{2+}]_{cyt}$ elevation in ABA signal pathway in arabidopsis guard cells. *Plant Cell Physiol.* **60**, 1146–1159 (2019).
75. Y. Ito, H. Kaku, N. Shibuya, Identification of a high-affinity binding protein for N-acetylchitooligosaccharide elicitor in the plasma membrane of suspension-cultured rice cells by affinity labeling. *Plant J.* **12**, 347–356 (1997).
76. H. Kaku *et al*., Plant cells recognize chitin fragments for defense signaling through a plasma membrane receptor. *Proc. Natl. Acad. Sci. U.S.A.* **103**, 11086–11091 (2006).
77. M. Hayafune *et al*., Chitin-induced activation of immune signaling by the rice receptor CEBiP relies on a unique sandwich-type dimerization. *Proc. Natl. Acad. Sci. U.S.A.* **111**, E404–E413 (2014).
78. T. Shinya *et al*., Functional characterization of CEBiP and CERK1 homologs in arabidopsis and rice reveals the presence of different chitin receptor systems in plants. *Plant Cell Physiol.* **53**, 1696–1706 (2012).
79. K. Ueno, T. Kinoshita, S. Inoue, T. Emi, K. Shimazaki, Biochemical characterization of plasma membrane H^+-ATPase activation in guard cell protoplasts of Arabidopsis thaliana in response to blue light. *Plant Cell Physiol.* **46**, 955–963 (2005).